Boundary Control Synthesis for a Lithium-Ion Battery Thermal Regulation Problem

James Ng and Stevan Dubljevic
Dept. of Chemical and Materials Engineering, University of Alberta, Edmonton, AB, Canada

DOI 10.1002/aic.14183
Published online July 29, 2013 in Wiley Online Library (wileyonlinelibrary.com)

The thermal regulation problem for a lithium ion (Li-ion) battery with boundary control actuation is considered. The model of the transient temperature dynamics of the battery is given by a nonhomogeneous parabolic partial differential equation (PDE) on a two-dimensional spatial domain which accounts for the time-varying heat generation during the battery discharge cycle. The spatial domain is given as a disk with radial and angular coordinates which captures the nonradially symmetric heat-transfer phenomena due to the application of the control input along a portion of the spatial domain boundary. The Li-ion battery model is formulated within an appropriately defined infinite-dimensional function space setting which is suitable for spectral controller synthesis. The key challenges in the output feedback model-based controller design addressed in this work are: the dependence of the state on time-varying system parameters, the restriction of the input along a portion of the battery domain boundary, the observer-based optimal boundary control design where the separation principle is utilized to demonstrate the stability of the closed loop system, and the realization of the outback feedback control problem based on state measurement and interpolation of the temperature field. Numerical results for simulation case studies are presented. © 2013 American Institute of Chemical Engineers *AIChE J*, 59: 3782–3796, 2013

Keywords: Li-ion battery, thermal regulation, parabolic PDE, distributed parameter systems, nonautonomous systems, boundary control, observer design, output feedback control

Introduction

The development of Lithium-ion (Li-ion) battery technology is one of the most important fields in the emerging global market for advanced energy storage devices, and there continues to be an intensive research effort within this area to meet the current and future demands of consumers and industry which utilize this technology. Presently, Li-ion battery technology has been widely adopted for use in personal electronics, and is also the most promising candidate for use in electric vehicles (EVs) and hybrid electric vehicles (HEVs), because of their advantageous characteristics in terms of energy density, capacity, voltage, charge retention, low self-discharge rate, and stability, compared to other rechargeable types such as lead–acid, nickel–metal hydride, or zinc–halogen batteries.[1] One of the key issues in the application of the technology to high-performance electronic devices, HEVs, and EVs, is battery thermal management. At high-discharge rates, Li-ion batteries generate a significant amount of heat which can detrimentally affect the overall performance of the devices. Excessive heat and uneven temperature distributions prolonged over time can cause damage to the battery resulting in decreases in capacity, charge retention, battery lifespan, and physical deformations of the battery itself. Under more extreme conditions, the battery can undergo thermal runaway, which may result in the rupture of the battery casing, explosion, and ignition of the flammable electrolytes.[2,3]

There is a large amount of literature focused on the thermal analysis of Li-ion batteries which employ experimental and computation techniques to model the complex electrochemical reactions responsible for heat generation under a variety of operating conditions.[4–6] In conjunction with these studies, there are complementary works discussing various approaches in the thermal management of Li-ion batteries.[1,7] The primary means of temperature regulation are typically through exclusive and combinations of passive and active control strategies each involving air for heating/cooling, liquid for heating/cooling, and also the use of phase change materials (PCMs). The implementation of any of the aforementioned control methods is dependent on a number of factors including the battery system setup (e.g., single cell, battery pack, and shape), which affects the feasibility of heating/cooling system design. In all cases, model-based control design has the potential of enhancing these existing methodologies by improving controller performance.

Control design based on lumped-parameter models of systems has been widely adopted in industry and successfully applied to many chemical and materials engineering processes. On the other hand, control design methods based on PDE models, while less popular, are advantageous for processes such as the regulation of the temperature distribution in Li-ion batteries in which the distribution of the state is a critical factor. There are several approaches to the PDE

Correspondence concerning this article should be addressed to S. Dubljevic at stevan.dubljevic@ualberta.ca

model-based control design such as modal analysis and early lumping methods,[8] proper orthogonal decomposition,[9] backstepping methods,[10,11] and other methods including the use of infinite-dimensional systems theory.[12–16] While each differ in the abstract representation of the physical system, all of the approaches face similar challenges in terms of fundamental control concepts such as stabilization, optimality, state measurement, and observer design. These mathematical issues must be reconciled with practical considerations such as the placement of actuators and sensors, despite the added complexity even in considering simplified linear PDEs models in higher spatial dimensions.

In this work, we focus on the model-based control design for a Li-ion battery thermal regulation problem. The dynamics of the battery temperature distribution are modeled by a linear nonhomogeneous parabolic PDE on a two-dimensional (2-D) spatial domain given as a disk region with radial and angular coordinates. We consider the case in which controller action is restricted to a portion of the boundary, which reflects more realistic thermal management system design considerations where physical limitations prohibit the placement of internal actuators in the battery cell itself, or along the entire boundary. The nonradially symmetric temperature distribution due to the application of the control input along a portion of the spatial domain boundary also provides a clearer picture of the heat-transfer phenomena for the thermal regulation problem. The approach to the controller design is based on the infinite-dimensional system representation of the PDE boundary control problem.[15,17–20] There are several key challenges in this context with regards to the model and system setup considered in this work. First, time-varying state (temperature) dependent and state independent heat generation terms, due to the underlying exothermic electrochemical reactions, are present in the model and are sources of instability which must be properly regulated by the controller. Second, the restriction of the input to a portion of the boundary represents a boundary control problem and requires the reformulation of the system for the purpose of controller design. The third primary challenge is the state measurement problem. In practice, the temperature distribution of the whole system is not directly known and must be estimated by measurements taken at the boundary of the system, and/or measurements by sensors located at points within the domain from which the temperature field can then be approximated. We provide the observer-based control formulation for the boundary control problem and demonstrate that the stability of the closed loop system is achieved by the optimal design of the controller and observer gain operators using the separation principle for the boundary control system. As an alternative approach, we also provide the output feedback control design based on the combined use of static measurements and interpolation of the temperature field which provides a robust and physically realizable pragmatic method for the realization of the Li-ion battery thermal regulation boundary control problem.

This article is organized as follows: The next section provides an overview of the PDE model of the battery temperature dynamics. The following section deals with the infinite-dimensional system representation of the boundary control problem which yields a suitable form for the state estimation and output feedback controller design described in section State Estimation and Output Feedback Control. The next section provides numerical simulation results for a set of case studies carried out to compare the controller formulation under different tuning parameters and the overall behavior of the closed loop feedback system.

Model Description

Li-ion batteries consist of three primary active components: a carbon anode, a metal oxide cathode, and a lithium salt in an organic solvent which serves as the electrolyte, and a nonactive current collection component. The anode and the cathode are separated by a thin sheet of microperforated plastic which prevents contact between the positive and negative electrodes while allowing ions to pass through. During the charging of the battery, lithium ions move from the cathode to the anode, and vise versa during the discharging of the battery, electrons travel through an external circuit which produces an electrical current through the collection layer, and heat within the battery enclosure is generated by the combination of this flow of electrons along with entropy changes of each of the reactive species. The electrochemical reactions during the charging and discharging of the battery are described by a set of half-reactions which occur at the cathode and anode. For a Li-ion battery which uses lithium-nickel-manganese-cobalt-oxide ($LiNiMn_2CoO_2$) as the cathode material, the cathode half reaction is

$$Li_{0.5}CoO_2 + xLi^+ + xe^- \underset{\text{charge}}{\overset{\text{discharge}}{\rightleftharpoons}} Li_{0.5+x}CoO_2$$

The anode half reaction is

$$LiC_6 \underset{\text{charge}}{\overset{\text{discharge}}{\rightleftharpoons}} Li_{1-2x}C_6 + 2xLi^+ + 2xe^-$$

The overall reaction is given by

$$2Li_{0.5}CoO_2 + LiC_6 \underset{\text{charge}}{\overset{\text{discharge}}{\rightleftharpoons}} 2Li_{0.5+x}CoO_2 + Li_{1-2x}C_6$$

The entropy changes of each of $LiNiMnCoO_2$, LiC_6, and $LiCoO_2$ have been experimentally determined as functions of the battery cell state of charge (SOC), and the current i, and are dependent on time according to the known battery rate of discharge.[21–23] The SOC refers to the chemical oxidation state of the active materials in the battery system which is measured as a fraction of the maximum capacity. The SOC decreases as the battery is discharged, and increases during charging. The rate of discharge relative to the maximum capacity is measured in terms of the C-rate. During thermal testing, batteries are discharged at various C-rates, and the surface temperatures are measured to determine the entropy changes, $S_\Delta(t)$, in terms of the SOC with respect to the rate at which the battery is discharged.* The model of the battery temperature dynamics in this section is given in Ref. 24 and references therein. In particular, $S_\Delta(t)$ is obtained from experimental studies, cited in that paper, of the particular battery system at a specified discharge rate which provide *a priori* knowledge of the time-dependent heat generation terms of the PDE model such that no online estimation of the associated entropy changes are required in the controller design considered in this work. On the other

*For example, a 1C rate implies that the chosen discharge current will deplete the battery charge in 1 h. A battery with a 100 Amp-h capacity rating is discharged at a current of 100 A (i.e., at a 1C discharge rate), such that the SOC at the 30-min mark is 0.5.

hand, online estimates of the rate of heat release can easily be combined with the approach taken in this current article. The model and subsequent controller design are also appropriate for use in describing the temperature dynamics during discharge–recharge cycling by extension of the experimental results to provide $S_\Delta(t)$ for the battery discharge–recharge cycle. However, this current article will only focus on the thermal regulation problem for the discharge part of the cycle.

The energy balance model for the transient temperature $Z(\xi,t)$ in a spatial region $\Omega \in \mathbb{R}^N$ with points ξ, and boundary $\partial\Omega$, is described by the parabolic PDE

$$\begin{aligned} \rho C_p \frac{\partial Z}{\partial t} &= \nabla \cdot (K_0 \nabla Z) + \dot{Q}(Z,\xi,t), \quad \text{for} \quad \xi \in \Omega, \quad t \in (0,T] \\ -K_0 \frac{\partial Z}{\partial n} &= h(Z - Z_a), \qquad\qquad \text{for} \quad \xi \in \partial\Omega, \quad t \in (0,T] \end{aligned} \tag{1}$$

where ∇ is the gradient operator. The index T denotes the time at which the battery is depleted (SOC = 0). The heat generation term $\dot{Q}$ is given by

$$\dot{Q} = \frac{i^2}{\sigma_{\text{con}}} - Z S_\Delta(t) \frac{i}{n_R F}, \qquad \text{for} \qquad S_\Delta(t) = \sum_k S_{\Delta,k}(t) \tag{2}$$

where $S_{\Delta,k}(t)$ is the entropy change for the kth species shown in the Figure 1.[24] It will be convenient to work with the dimensionless form of the problem for the remainder of this work. Normalization with $\tilde{t} = t\kappa/|\xi|^2$, $\tilde{\xi} = \xi/|\xi|$, $z(\xi,t) = (Z - Z_a)/Z_a$, and dropping the tildes yields the dimensionless form of the PDE

$$\begin{aligned} \frac{\partial z}{\partial t} &= \nabla^2 z + g(t) z + q(t) \quad \text{for} \quad \xi \in \Omega, \quad t \in (0,T] \\ -\beta \nabla z &= z \qquad\qquad\qquad\quad \text{for} \quad \xi \in \partial\Omega, \quad t \in (0,T] \end{aligned} \tag{3}$$

where $\kappa = K_0/\rho C_p$, $g(t) = -S_\Delta(t) i V Z_a^2/n_R F K_0$, $q(t) = Z_a V i^2/K_0 \sigma_{\text{extcon}} - S_\Delta(t) Z_a^2 V i/n_R F K_0$, and $\beta = K_0/h Z_a^2$.

Li-ion battery units are manufactured in a variety of configurations with various geometries including rectangular parallel-piped and cylindrical forms. Batteries with cylindrical geometry are constructed with thin layers of the cathode, separator, current collector, and anode, which are spirally wound and inserted into a cylindrical can. The battery geometry considered for the remainder of this work is the unit disk depicted in Figure 2 where $\xi = (r,\theta)$, $0 \le r \le 1$, $-\pi \le \theta \le \pi$, and $\Omega := (0,1) \times (-\pi,\pi)$ where the spirally wound layers make up the homogeneous disk region. The physical properties of the battery are taken according to the proportion of each component present in the battery, see Table 4.[24] Although the disk itself is taken to be radially symmetric, we do not assume the temperature distribution of the disk to be radially symmetric. The PDE system is then given by

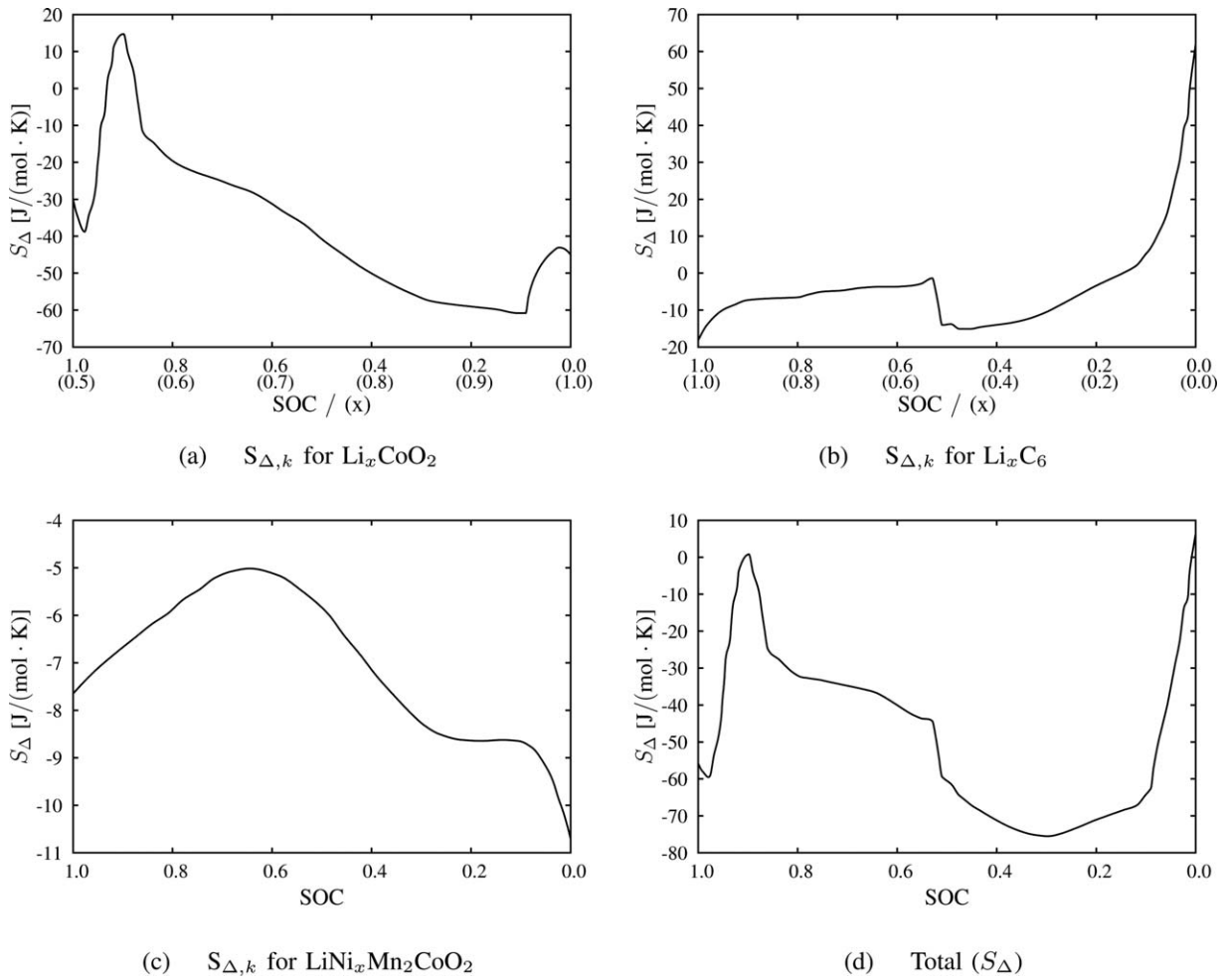

Figure 1. Entropy changes for $LiCoO_2$, LiC_6, $LiNiMn_2CoO_2$, and the total entropy change ΔS, as functions of the state of charge (SOC).[24]

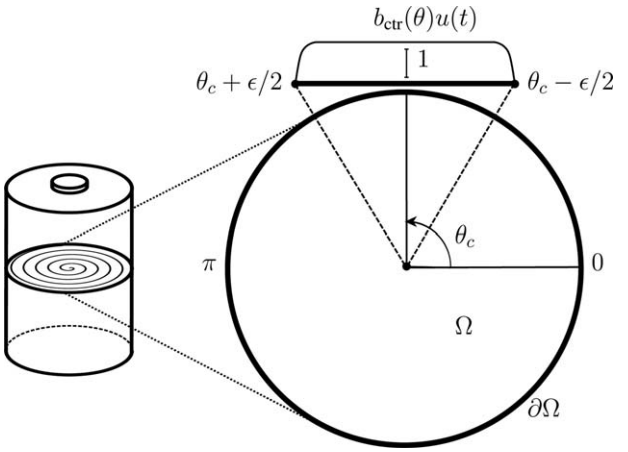

Figure 2. Battery system schematic with boundary actuation.

$$\begin{aligned}&\frac{\partial z}{\partial t}=A(r,\theta,t)z+q(t), && (r,\theta)\in\Omega, && t\in(0,T]\\ &z(r,\theta,0)=z_0(r,\theta), && (r,\theta)\in\Omega, && t=0\end{aligned} \tag{4}$$

where z_0 is the initial condition and the operator $A(r,\theta,t)$ is defined as

$$A(r,\theta,t)=\frac{1}{r}\frac{\partial}{\partial r}\left(r\frac{\partial}{\partial r}\right)+\frac{1}{r^2}\frac{\partial^2}{\partial\theta^2}+g(t) \tag{5}$$

The boundary conditions are given by

$$\begin{aligned}&z(r,-\pi,t)=z(r,\pi,t), \quad \frac{\partial z}{\partial\theta}(r,-\pi,\theta)=\frac{\partial z}{\partial\theta}(r,\pi,t),\\ &\quad 0<r<1, \quad t\in(0,T]\\ &\frac{\partial z}{\partial r}(0,\theta,t)=0, \quad \beta\frac{\partial z}{\partial r}(1,\theta,t)+z(1,\theta,t)=b_{\text{ctr}}(\theta)u(t),\\ &\quad -\pi<\theta<\pi, \quad t\in(0,T]\end{aligned} \tag{6}$$

where $z(r,\theta,t)$ is bounded at the origin $r=0$, that is, $|z(0,\theta,t)|<\infty$. As previously mentioned, in many applications, physical limitations may prohibit the input from being applied to the entire domain boundary. To reflect this restriction, we consider the case in which the input is applied at $r=1$ over a region of the boundary $\epsilon\in(-\pi,\pi)$ and centered at θ_{ctr} as depicted in Figure 2 such that

$$b_{\text{ctr}}(\theta)u(t)=\begin{cases}u(t) & \text{for} \quad \theta\in[\theta_{\text{ctr}}-\epsilon/2,\theta_{\text{ctr}}+\epsilon/2]\\ 0 & \text{for} \quad \theta\notin[\theta_{\text{ctr}}-\epsilon/2,\theta_{\text{ctr}}+\epsilon/2]\end{cases} \tag{7}$$

In this form, the function $b_{\text{ctr}}(\theta)=H(\theta-(\theta_{\text{ctr}}-\epsilon/2))-H(\theta-(\theta_{\text{ctr}}+\epsilon/2))$, where $H(\theta)$ is the Heaviside step function, and has discontinuities at $\theta=\theta_{\text{ctr}}-\epsilon/2$ and $\theta=\theta_{\text{ctr}}+\epsilon/2$. In practice, it is usually not possible for the input to be uniformly applied over the interval. Also, $dH(\theta)/d\theta=\delta(\theta)$, where $\delta(\theta)$, which is the delta function, is not differentiable which introduces some mathematical technicalities. In particular, the formulation of the control problem will require a continuous second-order derivative of $b(\theta)$. A more realistic assumption which remedies both the practical and technical issues which is utilized in this work is where $b_{\text{ctr}}(\theta)$ is given by

$$b_{\text{ctr}}(\theta)=\begin{cases}\dfrac{1}{1+e^{-2K_1(\theta-\theta_{\text{ctr}}+\epsilon/2)}}-\dfrac{1}{1+e^{-2K_1(\theta-\theta_{\text{ctr}}-\epsilon/2)}} & \text{for} \quad \theta\in[\theta_{\text{ctr}}-\epsilon/2,\theta_{\text{ctr}}+\epsilon/2]\\ 0 & \text{for} \quad \theta\notin[\theta_{\text{ctr}}-\epsilon/2,\theta_{\text{ctr}}+\epsilon/2]\end{cases} \tag{8}$$

The functions in Eq. 8 approximating the Heaviside functions are referred to as logistic functions where the parameter K_1 affects how steeply the function increases and decreases, and have continuous second-order derivatives. One can view $b_{\text{ctr}}(\theta)$ as a type of shaping function which determines the range and "shape" by which the input is applied on the boundary.

Boundary Control and Infinite-Dimensional System Representation

The PDE system in Eqs. 4–6 represents a boundary control problem where the input appears as an inhomogeneous term in the boundary condition. In this section, the problem is reformulated by means of a state transformation such that the resulting system has homogeneous boundary conditions. The corresponding infinite-dimensional system representation of the problem as an abstract evolution system on a Hilbert space is then provided. Consider the transformation by defining the new variable

$$v(r,\theta,t)=z-b(r,\theta)u(t), \quad \text{where} \quad b(r,\theta)=b_{\text{ctr}}(\theta)\frac{r^2}{2\beta+1} \tag{9}$$

such that $b(r,\theta)u(t)$ satisfies the radial boundary conditions. The initial and boundary control problem in Eqs. 4–6 is transformed to the PDE system in terms of v with homogeneous boundary conditions

$$\begin{aligned}&\frac{\partial v}{\partial t}=A(r,\theta,t)v-b(r,\theta)\dot{u}(t)+A(r,\theta,t)b(r,\theta)u(t)+q(t),\\ &\quad v(r,\theta,0)=v_0(r,\theta) \quad v(r,-\pi,t)=v(r,\pi,t),\\ &\quad \frac{\partial v}{\partial\theta}(r,-\pi,t)=\frac{\partial v}{\partial\theta}(r,\pi,t)\frac{\partial v}{\partial r}(0,\theta)=0,\\ &\quad \beta\frac{\partial v}{\partial r}(1,\theta)+v(1,\theta)=0\end{aligned} \tag{10}$$

where $A(r,\theta,t)$ is given in Eq. 5 and

$$A(r,\theta,t)b(r,\theta)u(t)=\frac{b_{\text{ctr}}(\theta)}{2\beta+1}\left(4+\mu(\theta)+r^2g(t)\right)u(t), \quad \text{with}$$
$$\mu(\theta)=b_{\text{ctr}}^{-1}(\theta)\frac{d^2b_{\text{ctr}}}{d\theta^2} \tag{11}$$

One can note that for $\theta\notin[\theta_{\text{ctr}}-\epsilon/2,\theta_{\text{ctr}}+\epsilon/2]$, the function determining the boundary region on which the input is

applied becomes $b_{\mathrm{ctr}}(\theta)=0$, so that $v(r,\theta,t)=z(r,\theta,t)$, which corresponds to the PDE system in Eqs. 4–6.

The Fourier–Bessel expansion of the initial data $v_0(r,\theta)$ is given in terms of the double set of eigenfunctions $\phi_{mn}^{(1)}$ and $\phi_{mn}^{(2)}$ of $A(r,\theta,t)$ where

$$v(r,\theta,0)=\sum_{m=0,n=1}^{\infty}\left(A_{mn}\phi_{mn}^{(1)}+B_{mn}\phi_{mn}^{(2)}\right)=v_0(r,\theta) \tag{12}$$

The eigenfunctions obtained from the nontrivial eigenvalue problem for $A(r,\theta,t)$ are expressed as the combination of Bessel functions and trigonometric functions where $J_m(\alpha_{m,n}r)$, $m=0,1,2,\ldots$, $n=1,2,\ldots$ are Bessel functions of the first kind of order m, and where $\phi_{mn}^{(1)}$ and $\phi_{mn}^{(2)}$ are given by

$$\begin{aligned}\phi_{mn}^{(1)}&=\sqrt{\frac{2}{\pi}}\frac{J_m(\alpha_{m,n}r)}{|J_{m+1}(\alpha_{m,n})|}\cos(m\theta), \quad \text{and}\\ \phi_{mn}^{(2)}&=\sqrt{\frac{2}{\pi}}\frac{J_m(\alpha_{m,n}r)}{|J_{m+1}(\alpha_{m,n})|}\sin(m\theta)\end{aligned} \tag{13}$$

The zeros the Bessel functions denoted by $\alpha_{m,n}$ determined from the transcendental equation

$$\frac{\beta}{2}\left(J_{m-1}(\alpha_{m,n})-J_{m+1}(\alpha_{m,n})\right)+J_m(\alpha_{m,n})=0 \tag{14}$$

The coefficients A_{mn} and B_{mn} are determined using orthogonality relations with

$$\begin{aligned}A_{mn}&=\sqrt{\frac{2}{\pi}}\frac{1}{|J_{m+1}(\alpha_{m,n})|}\int_{\Omega}v_0(r,\theta)J_m(\alpha_{m,n}r)r\cos(m\theta)d\theta dr\\ &=\langle v_0,\psi_{mn}^{(1)}\rangle\\ B_{mn}&=\sqrt{\frac{2}{\pi}}\frac{1}{|J_{m+1}(\alpha_{m,n})|}\int_{\Omega}v_0(r,\theta)J_m(\alpha_{m,n}r)r\sin(m\theta)d\theta dr\\ &=\langle v_0,\psi_{mn}^{(2)}\rangle\end{aligned} \tag{15}$$

The adjoints $\psi_{mn}^{(i)}$ $(i=1,2)$ are orthonormal to the respective $\phi_{mn}^{(i)}$, $i=1,2$ in Eq. 13, that is, for $m,k\geq 0$ and $n,l\geq 1$

$$\langle\phi_{mn}^{(i)},\psi_{kl}^{(i)}\rangle=\delta_{mk}\delta_{nl} \tag{16}$$

The zeros of the Bessel function $\alpha_{m,n}>0$ for $m=0,n\geq 1$ are simple and correspond to radially symmetric eigenfunctions, while $\alpha_{m,n}>0$ for $m\geq 1,n\geq 1$ forms a double set and corresponds to a double of linearly independent eigenfunctions with dependence on the angular variable. Together, the eigenfunctions $\phi_{mn}^{(i)}$ and $\psi_{mn}^{(i)}$ form an orthonormal basis of the Hilbert space $L^2(\Omega)$ on which any $z(r,\theta,t)\in L^2(\Omega)$ can be represented by an infinite Fourier–Bessel series expansion.

Infinite-dimensional system representation

The thermal regulation problem, specifically the PDE model of the battery temperature dynamics, can be represented as an abstract initial value problem on an infinite-dimensional state space of functions which is analogous to the representation of ordinary differential equations on a finite-dimensional vector space. Moreover, this type of representation provides a convenient form to study the dynamics of the system and also to consider the output feedback controller design problem. Let us briefly depart from the battery thermal regulation problem and introduce the function space setting in which the infinite-dimensional system representation of the boundary control problem is considered.

Let Ω be a spatial domain in $\mathbb{R}^N$ with points ξ, volume element dv, and boundary $\partial\Omega$. The letters $s,t\in[0,T]$ will denote the time indices where $0\leq s\leq t\leq T<\infty$. General Banach spaces will be denoted by the calligraphic letters, for example, $\mathcal{Z}$ with norm $||\cdot||$. The set of bounded linear operators $F:\mathcal{Z}\to\mathcal{Y}$ is denoted $\mathcal{L}(\mathcal{Z},\mathcal{Y})$, and $F:\mathcal{Z}\to\mathcal{Z}$ as $\mathcal{L}(\mathcal{Z})$. For functions $z\in Z$, we denote $C([0,T];\mathcal{Z})$ as the class of all continuously differentiable functions defined for $t\in[0,T]$ and taking values in $\mathcal{Z}$. The space $L^2(\Omega)$ is the standard space of square integrable functions, and is a Hilbert space with the inner product $\langle u,v\rangle=\int_{\Omega}u(\xi)v(\xi)dv$.[18] For time-dependent functions, we denote $L^2([0,T];\mathcal{Z})$ as the set of all functions z taking values in $\mathcal{Z}$ and $||z(\xi,t)||_{\mathcal{Z}}^2$ square integrable in $[0,T]$ with the norm $||z||_{L^2([0,T];\mathcal{Z})}=\left(\int_0^T||z(\xi,t)||_{\mathcal{Z}}^2dt\right)^{1/2}$. Unless specified otherwise, we denote $||\cdot||$ as the $L^2(\Omega)$ norm.

Parabolic PDEs can be represented in this function space setting as general abstract initial value problems in the form

$$\dot{z}(t)=A(t)z(t),\quad z(0)=z_0 \tag{17}$$

where the nonautonomous operator $A(t)$ is associated with the PDE spatial operator and a domain $D(A(t))$ densely defined in the state space $\mathcal{Z}$, which is usually a Hilbert space.[17,19] The solution of initial value problems with nonautonomous operators as in Eq. 17 are expressed in terms of two-parameter semigroups which determine the evolution of the state on $\mathcal{Z}$. Formally, we define this operator as follows [Ref. 17, Theorem, 6.1, Chapter 5.6].

Definition 1. A two-parameter semigroup $U(t,s)$, $0\leq s\leq t\leq T$ is a family of bounded linear operators on $\mathcal{Z}$ which satisfies: (i) $||U(t,s)||\leq C$ where C is a positive constant; (ii) $(t,s)\to U(t,s)$ is continuous in the uniform operator topology; and (iii) for $0\leq s\leq\tau\leq t\leq T$, we have $U(t,t)=I$, $U(t,s)=U(t,\tau)U(\tau,s)$, and

$$\frac{\partial U(t,s)}{\partial t}=A(t)U(t,s),\quad \frac{\partial U(t,s)}{\partial s}=-U(t,s)A(s)$$

The two-parameter semigroup $U(t,s)$ is often referred to as an evolution operator due to the property (iii) in Definition 1. The solution of the initial value problem in Eq. 17 is expressed in terms of this operator

$$z(t)=U(t,s)z_s,\quad z(s)=z_s\quad 0\leq s\leq t\leq T \tag{18}$$

Remark 1. As a brief example, consider the distributed control problem for the one-dimensional heat equation on the domain $\Omega:=[0,1]$

$$\begin{aligned}&\frac{\partial z}{\partial t}=\alpha(t)\frac{\partial^2 z}{\partial\xi^2}+u(\xi,t),\quad z(\xi,0)=z_0(\xi),\\ &\frac{\partial z}{\partial\xi}(0,t)=0=\frac{\partial z}{\partial\xi}(1,t)\end{aligned} \tag{19}$$

where $u(\xi,t)$ is the input distributed over Ω. The time-dependent coefficient $\alpha(t)$ describes processes in which the conductivity or diffusivity changes over time, for example,

where catalyst activation/deactivation is present,[25] and in models of moisture sorption in composite materials.[26] Assume first that $u(\xi,t)=0$. The solution $z(\xi,t)$ is given by

$$z(\xi,t)=U(t,0)z_0=\sum_{n=0}^{\infty} e^{\int_0^t \lambda_n(\tau)d\tau}\langle z_0(\xi),\phi_n(\xi)\rangle\phi_n(\xi) \tag{20}$$

where $\phi_n(\xi)=\sqrt{2}\cos(n\pi\xi)$ are the eigenfunctions and $\lambda_n(t)=-\alpha(t)(n\pi)^2$ are the eigenvalues. The PDE in Eq. 19 can also be represented as the evolution system $\dot{z}(t)=A(t)z(t)+Bu(t)$ on the state space $\mathcal{Z}=L^2([0,1])$, where $A(t)z=\alpha(t)\left(\partial^2 z/\partial\xi^2\right)$ and $B=I$. Note that the eigenfunctions form an orthonormal basis of $\mathcal{Z}$. Defining the state $z(t):=[z(\xi)](t)$, the solution of Eq. 19 is expressed as

$$z(t)=U(t,0)z_0+\int_0^t U(t,\tau)u(\tau)d\tau$$

where the operator $U(t,s),\ 0\le s\le t\le T$ is the two-parameter semigroup which describes the state evolution on $\mathcal{Z}$ from any initial state $z_s\in L^2(\Omega)$ and is given by (cf. Eq. 20)

$$U(t,s)z_s=\sum_{n=0}^{\infty} e^{\int_s^t \lambda_n(\tau)d\tau}\langle z_s,\phi_n\rangle\phi_n \tag{21}$$

One can verify that the operator in Eq. 21 satisfies the properties in Definition 1.

The following section deals with the representation of the battery thermal regulation problem within this infinite-dimensional systems framework. The use of boundary actuation to control the temperature requires some modification to the above procedure. Specifically, one considers the transformation of $z(r,\theta,t)$ in the original PDE system in terms of $v(r,\theta,t)$ given in Eq. 9.

Boundary control formulation as an infinite-dimensional system

Consider the boundary control problem on the state space $\mathcal{Z}=L^2(\Omega)$ with states $z(t)=[z(r,\theta)](t)$ such that the system in Eqs. 4–6 is represented as the initial value problem

$$\dot{z}(t)=\mathfrak{A}(t)z(t)+q(t),\quad z(0)=z_0,\quad \mathfrak{B}z(t)=b_{\text{ctr}}u(t) \tag{22}$$

with nonautonomous differential operator $\mathfrak{A}(t)=A(r,\theta,t)$

$$\mathfrak{A}(t):=\frac{1}{r}\frac{\partial}{\partial r}\left(r\frac{\partial}{\partial r}\right)+\frac{1}{r^2}\frac{\partial^2}{\partial\theta^2}+g(t) \tag{23}$$

The domain $D(\mathfrak{A}(t))\subset\mathcal{Z}$ is defined as

$$D(\mathfrak{A}(t))=\left\{z\in\mathcal{Z}\,\middle|\, z,\frac{\partial z}{\partial r},\frac{\partial z}{\partial\theta}\text{ are a.c., }\frac{\partial^2 z}{\partial r^2},\frac{\partial^2 z}{\partial\theta^2}\in\mathcal{Z},\ \text{and }\frac{\partial z}{\partial r}(0,\theta,t)=0\right\} \tag{24}$$

The boundary operator $\mathfrak{B}:\mathcal{Z}\to\mathbb{R}$ is defined as

$$\mathfrak{B}z=\beta\frac{\partial z}{\partial r}(1,\theta,t)+z(1,\theta,t),\quad D(\mathfrak{A}(t))\subset D(\mathfrak{B}) \tag{25}$$

Let us define the associated operator $A(t)$ on $\mathcal{Z}$ with domain $D(A(t))=D(\mathfrak{A})\cap\ker\mathfrak{B}=\{z\in D(\mathfrak{A}(t))/\mathfrak{B}z=0\}$ given by

$$D(A(t))=\left\{z\in\quad \mathrm{Z}\,\middle|\, z,\frac{\partial z}{\partial r},\frac{\partial z}{\partial\theta}\text{are a.c.},\frac{\partial^2 z}{\partial r^2},\frac{\partial^2 z}{\partial\theta^2}\in\mathcal{Z},\ \text{and }\frac{\partial z}{\partial r}(0,\theta,t)=0,\beta\frac{\partial z}{\partial r}(1,\theta,t)+z(1,\theta,t)=0\right\}$$
$$\text{with } A(t)z(t)=\mathfrak{A}(t)z(t)\text{ in } D(A(t)) \tag{26}$$

Let $B=[b(r,\theta)]=b_{\text{ctr}}(\theta)r^2/(2\beta+1)$, where $B\in L^2(\Omega)$ is continuous and bounded for all $r,\theta\in\Omega$ and satisfies

$$\mathfrak{B}(Bu(t))=b_{\text{ctr}}(\theta)u(t),\quad \text{for all}\quad u(t)\in\mathbb{R} \tag{27}$$

Using the transformation in Eq. 9 with $v(t)=z(t)-Bu(t)$, the boundary control problem for the PDE system in Eq. 10 is represented as the nonautonomous infinite-dimensional system with state $v(t)=[v(r,\theta)](t)$

$$\dot{v}(t)=A(t)v(t)-B\dot{u}(t)+\mathfrak{A}(t)Bu(t)+q(t) \tag{28}$$

The operator $A(t)$, $0\le s<t\le T$, is given by

$$A(t)v(t)=\sum_{m=0,n=1}^{\infty}\lambda_{mn}(t)\langle v(t),\psi_{mn}\rangle\phi_{mn}$$

where

$$\lambda_{mn}(t)=-\alpha_{m,n}^2+g(t),\quad \psi_{mn}=\begin{pmatrix}\psi_{mn}^{(1)}\\ \\ \psi_{mn}^{(2)}\end{pmatrix},\quad\text{and} \tag{29}$$

$$\phi_{mn}=\begin{pmatrix}\phi_{mn}^{(1)}\\ \\ \phi_{mn}^{(2)}\end{pmatrix}$$

The operator $A(t)$ generates the two-parameter semigroup $U(t,s)$, $0\le s\le t\le T$ given by

$$U(t,s)v(s)=\sum_{m=0,n=1}^{\infty}\exp\left\{\int_s^t\lambda_{mn}(\tau)d\tau\right\}\langle v(s),\psi_{mn}\rangle\phi_{mn} \tag{30}$$

The analytic form of the two-parameter semigroup generated by the nonautonomous operator $A(t)$ resembles the form of the standard one-parameter semigroups generated by analogous autonomous operators on a Hilbert space.[15] One can note that for each $t\in[0,T]$, the operator $A(t)$ is the infinitesimal generator of an analytic semigroup $S_t(s), s\ge 0$.[17] For all $t\in 0\le s\le t\le T$, the operator $U(t,s)$ determines the state evolution according to the previous definition.

Proposition 1. The operator $U(t,s)$ in Eq. 30 satisfies (i)–(iii) of Definition 1.

The proof of Proposition 1 is provided in the Appendix. The solution of the initial value problem corresponding to the transformed system in Eq. 28 is expressed as

$$v(t)=U(t,s)v_s-\int_s^t U(t,\tau)B\dot{u}(\tau)d\tau+\int_s^t U(t,\tau)\mathfrak{A}(\tau)Bu(\tau)d\tau+\int_s^t U(t,\tau)q(\tau)d\tau \tag{31}$$

Then, the solution of the original system is given by

$$z(t)=Bu(t)-U(t,0)Bu(0)+U(t,0)z_0-\int_0^t U(t,\tau)B\dot{u}(\tau)d\tau+\int_0^t U(t,\tau)\mathfrak{A}(\tau)Bu(\tau)d\tau+\int_0^t U(t,\tau)q(\tau)d\tau \tag{32}$$

Equation 32 is provided in terms of the boundary input $u(t)$ as well as its derivative $\dot{u}(t)$. Problems of this type have been considered by extension of the state space to include the input space $\mathcal{U}$, that is, on the extended state space $\mathcal{Z}^e := L^2(\Omega) \oplus \mathbb{R}$. In this way, the controller design is based on the extended system which is driven by integral action via the derivative of the input $\dot{u}(t)$, and the input $u(t)$ is then determined by integration.[15] On the other hand, the controller can be designed based on the input itself provided that the system is well defined for $u(t) \in \mathcal{U}$ (in practice, the input space is typically defined as $\mathcal{U}=\mathbb{R}$), and square integrable over $t \in [0,T]$. This condition is formally stated by the following Proposition which will be utilized in the following sections in which the state estimation and controller design problems will be considered.

Proposition 2. The solution of the boundary control problem expressed in Eq. 32 is well defined for every input $u(t) \in L^2([0,T];\mathcal{U})$.

The proof of Proposition 2 is provided in the Appendix. Let us briefly summarize the procedure thus far before proceeding to the following sections. We have considered the PDE system in Eqs. 4–6 which has two distinguishing features: first, the presence of time-dependent generation terms, and second, the input is applied over a portion of the boundary. The transformation in Eq. 9 was utilized to convert the problem to a PDE system in Eq. 10 with homogeneous boundary conditions. Next, the infinite-dimensional system representation of the boundary control problem was considered on the state space $\mathcal{Z}=L^2(\Omega)$. The formal definition yielded the representation of the PDE in Eq. 10 as the nonautonomous infinite-dimensional system in Eq. 28. Utilizing the two-parameter semigroup given in Eq. 30, the solution of the nonautonomous infinite-dimensional system is given in Eq. 31. Finally, the solution of the original system is provided in Eq. 32. The following sections deal with the state estimation and output feedback control problem for the determination of the input.

Remark 2. One can notice that the time-dependence of the operator $A(t)$ is due to the generation term $g(t)$ associated with the state. For $g(t)=g$ (constant), the operator in Eq. 29 becomes

$$Av(t) = \sum_{m=0,n=1}^{\infty} \lambda_{mn} \langle v(t), \psi_{mn} \rangle \phi_{mn}, \quad \text{where} \quad \lambda_{mn} = -\alpha_{m,n}^2 + g, \tag{33}$$

which generates the analytic semigroup $S(t)$, $t \geq 0$

$$S(t-s)v(s) = \sum_{m=0,n=1}^{\infty} e^{\lambda_{mn}(t-s)} \langle v(s), \psi_{mn} \rangle \phi_{mn} \tag{34}$$

State Estimation and Output Feedback Control

The measurement of the battery temperature is a critical factor in the state estimation problem, the design to the control law, and the overall performance of the closed loop system. The true state (temperature distribution) must be estimated from a finite-number of sensors collecting information about the partial state of the system, for example, combinations of point, regional, boundary and in-domain temperature measurements.

Methods utilized to approximate the state must take into consideration physical design and practical limitations. From a battery engineering perspective, an ideal situation would be where the temperature measurements are noninvasive of the actual functional parts of the battery, that is, realized by placement of thermocouples which measure the temperature only on points or regions of the boundary. In some lumped-parameter models of the battery system, this approach is utilized.[27] However, as in the present context in which the temperature is assumed to be distributed, the restriction to boundary measurements represents a complex problem. From a mathematical control perspective, the approach to the state estimation and controller design problem is the construction of an observer. The case in which only boundary measurements are available inherits two primary challenges: first, the temperature of the system throughout of the domain must be reconstructed from the measured temperature available only on a portion(s) of the boundary, and therefore requires the determination of a relationship between the two; second, the relationship between the boundary and domain temperatures can only be developed from the state estimates of the system (along with state estimates or measured states available on the boundary) as the temperature of the actual system is not known *a priori*. Although there are some works on the recovery of the system state from boundary measurements, compensator design remains an active area of research in distributed parameter systems.[28,29]

A less restrictive set of problems exist for cases in which measurements of the temperature field are assumed to be available from embedded sensors. Usually, the sensor measurements are taken to be point or averaged readings over small increments, from which the partial state of the system is ascertained. This idea naturally leads to important questions pertaining to the number and optimal placement of sensors required to ensure that the system is (approximately) observable, detectable, stabilizable, etc., by checking rank conditions dependent on the sensor locations and definition of the measurement functions. From a control engineering perspective, one alternative to the state estimation problem is the use of point or regional sensors to reconstruct the temperature field by interpolation. An advantage of this approach is that it circumvents the need to design an observer, by using the reconstructed temperature field to obtain the state of the system which is then directly utilized in the controller design. This convenience comes at a cost of introducing computational overhead necessary to interpolate the temperature field from measurements, but this cost is offset as the method does not require an observer system to be run concurrent to the process. Moreover, the controller performance based directly on the measured states may be an improvement over the use of an observer system which requires the careful design of the observer gain such that the states converge to those of the actual system in a reasonable time to ensure the stability of the closed loop system. While the direct use of the measured states provides a more robust method for the feedback design problem, the accuracy of the estimation and state reconstruction also depends on the number and placement of the measurement locations. These ideas along with comparative cases will be discussed in further detail within later sections. In this section, we restrict our discussion and focus on first, the observer design method to demonstrate the dynamical properties of the closed loop output feedback system. Secondly, we consider the direct use of the state measurements for the state reconstruction via interpolation which will enable the practical realization of the output feedback boundary controlled battery temperature regulation problem.

Observer design

In practice, sensors are used to measure the temperature at points or regions which contain only partial information about the entire state of the system. The output $y(t)$ is given by

$$y(t)=Cz(t):=\int_{\Omega} c(r,\theta)z(r,\theta,t)drd\theta \tag{35}$$

The function $c(r,\theta)$ is approximated by the shape function around the measurement points $(r_i,\theta_i)\in\Omega,\ i=1,2,\ldots,n_{\mathrm{msr}}$ with $c(r,\theta)$ given by

$$c(r,\theta)=\frac{1}{4\zeta_1\zeta_2}\delta_{[r_i-\zeta_1,r_i+\zeta_1]}(r)\delta_{[\theta_i-\zeta_2,\theta_i+\zeta_2]}(\theta) \tag{36}$$

where $\delta_{[r_i-\zeta_1,r_i+\zeta_1]}(r)=1$ for $r_i-\zeta_1\le r\le r_i+\zeta_1$, and 0 otherwise (similarly, $\delta_{[\theta_i-\zeta_2,\theta_i+\zeta_2]}(\theta)$ is defined). In the case of a single temperature measurement, for example, C is a bounded linear operator $C\in\mathcal{L}(\mathcal{Z},\mathcal{Y})$ with the norm $1/\left(2\sqrt{\zeta_1\zeta_2}\right)$ and $\mathcal{Y}=\mathbb{R}$. Measurements on the boundary at $r=1$ and $\theta_j,\ j=1,2,\ldots,m_{\mathrm{msr}}$ can be approximated by the functions $c(1,\theta)=\delta_{\left[\theta_j-\zeta_2,\theta_j+\zeta_2\right]}(\theta)$, or analogous to the input function as in Eq. 8, taken from a region of the boundary $\eta\in(-\pi,\pi)$ centered at θ_{msr}. In the case of point measurements where $c(r,\theta)$ is given in Eq. 36, the compensator design problem for the boundary control system, as in Eq. 28, is given by

$$\dot{v}(t)=A(t)v(t)+\mathfrak{A}(t)Bu(t)-B\dot{u}(t)+q(t),\quad y(t)=Cv(t) \tag{37}$$

Recall from Proposition 2 that the solution of Eq. 37 is well defined for every $u(t)\in L^2([0,T];\mathcal{U})$ such that the control law can be determined based on the input, rather than its derivative, and denote this system by $\sum(A(t),\mathfrak{A}(t)B,C)$, which is assumed to be exponentially detectable. Consider a Luenberger observer for the system in Eq. 37 given by

$$\begin{aligned}\dot{\hat{v}}(t)&=A(t)\hat{v}(t)+\mathfrak{A}(t)Bu(t)-B\dot{u}(t)+q(t)-L(y(t)-\hat{y}(t)),\\ \hat{y}(t)&=C\hat{v}(t)\end{aligned} \tag{38}$$

where $\hat{v}(t)$ denotes the state estimates with initial condition $\hat{v}(0)=\hat{v}_0$ and $L\in\mathcal{L}(\mathrm{Y},\mathcal{Z})$ is the observer gain operator. The dynamics of the error $\varepsilon(t)=v(t)-\hat{v}(t)$ between the states $v(t)$ and the estimates $\hat{v}(t)$ are governed by the system

$$\dot{\varepsilon}(t)=(A(t)+LC)\varepsilon(t) \tag{39}$$

Note that the entropy-related generation term $g(t)\in C([0,T],\mathcal{Z})$ is bounded (see Figure 1) such that $||g(t)||\le k_g=\sup\{||g(t)||:t\in[0,T]\}$, and that the operator $A(t)$ in Eq. 26 can be seen as a perturbation of an autonomous operator A which is the infinitesimal generator of a strongly continuous semigroup $S_A(t),\ t\ge 0$. That is

$$A(t)=A+g(t),\quad \text{where}\quad g(t)v\in C([0,T];\mathcal{Z}) \tag{40}$$

The semigroup $S_A(t)$ is exponentially stable

$$||S(t)||\le Me^{\omega t},\quad \omega_0:=\sup_{m\ge 0,n\ge 1}\left(-\alpha_{mn}^2\right)\le\omega \tag{41}$$

where M is a generic positive constant, and $\omega<0$. By choosing the observer gain such that $k_g+||LC||=\gamma<0$, the operator $A(t)+LC$ generates the exponentially stable two-parameter semigroup $U_{LC}(t,s)$

$$||U_{LC}(t,s)||\le Me^{(\omega+\gamma)(t-s)} \tag{42}$$

Then, the solution of Eq. 39 is expressed as

$$\varepsilon(t)=U_{LC}(t,s)\varepsilon_0 \tag{43}$$

where $\varepsilon_0=v_0-\hat{v}_0$. As $U_{LC}(t,s)$ is exponentially stable, the error $\varepsilon(t)$ converges to zero as $t\to\infty$. Now, suppose for the moment that the nonhomogeneous generation term, independent of the state, is zero, that is, $q(t)=0$. Consider the input $u(t)=F\hat{v}(t)$ where $F\in\mathcal{L}(\mathcal{Z},\mathcal{U})$ feedback gain operator. The closed loop system for Eqs. 37 and 38 can be written together on the extended state space $\mathcal{Z}^e=\mathcal{Z}\oplus\mathcal{Z}$ as

$$\dot{v}^e(t)=A^e(t)v^e(t),\quad v^e(t)=\begin{pmatrix}v(t)\\ \hat{v}(t)\end{pmatrix}$$

and

$$A^e(t)=\begin{pmatrix}A(t)+BF(I+BF)^{-1}LC & \mathfrak{A}(t)BF-BF(I+BF)^{-1}(A(t)+LC+\mathfrak{A}(t)BF)\\ -(I+BF)^{-1}LC & (I+BF)^{-1}(A(t)+LC+\mathfrak{A}(t)BF)\end{pmatrix} \tag{44}$$

Utilizing the operator matrices $I_1=\begin{pmatrix}I & -I\\ 0 & I\end{pmatrix}$ and $I_2=\begin{pmatrix}I & I\\ 0 & I\end{pmatrix}$, the extended operator $A^e(t)$ is transformed to the following form

$$I_1A^e(t)I_2=\begin{pmatrix}A(t)+LC & 0\\ -(I+BF)^{-1}LC & (I+BF)^{-1}(A(t)+\mathfrak{A}(t)BF)\end{pmatrix} \tag{45}$$

The closed loop behavior of the output feedback system can be understood from Eq. 45 where the eigenspectrum of the closed loop system is given by $\sigma(A(t)+LC)\cup\sigma(A(t)+\mathfrak{A}(t)B)$. One can see that if L is chosen such that $A(t)+LC$ generates a stable two-parameter semigroup, then the choice of F such that $A(t)+\mathfrak{A}(t)BF$ generates an exponentially stable two-parameter semigroup also stabilizes the closed loop system. Each of the gain operators L and F can be designed optimally by considering the appropriate minimization problems.[15,30] One can note that the inclusion of the nonhomogeneous generation term $q(t)$ does not change the structure of Eq. 45, but appears as additional terms in Eq. 44 which are all independent of the state. An alternative approach to the stabilizing regulator design is by the conversion of the nonhomogeneous state equation in Eq. 37 into a homogeneous state equation via transformation. The associated optimization problem for the resulting homogeneous

system given in terms of the transformed state can then be considered [Ref. 30, Chapter 7.2, Part 4].

Interpolation-based output feedback controller design

Another approach toward the output feedback controller design is by directly utilizing the set of point or regional sensor measurements to reconstruct the entire temperature field by interpolation. That is, by utilizing the set of measurement points (r_i, θ_i) (and also (r_j, θ_j)), the temperature is approximated for all $(r, \theta) \in \Omega$ and $t \in [0, T]$ as $z(r, \theta, t) \approx \hat{z}(r, \theta, t)$, such that the output is given by $y(t) \approx \hat{z}(t) = \langle \hat{z}(r, \theta), \psi_{mn} \rangle$. One advantage of utilizing the temperature readings to interpolate the entire temperature field is that the output contains more information about the system than from individual temperature measurements, provided that the sensors are reasonably placed to capture the distribution. The logical choices of sensor locations in the present context of the battery control problem should reflect the axial symmetry of the domain and the expected dynamical behavior of the temperature evolution. For example, the temperature distribution in Figure 3a is reconstructed in Figure 3b by utilizing a total number of nine measurement locations, where $\{a, b, d, f\}$ are point measurements along the boundary, $\{g, h, i, j\}$ are taken along an intermediate ring at the interior of the domain, and the sensor $\{k\}$ is located at the center of the disk. Although the initial temperature distribution is not axisymmetric, one can note from modal analysis that the dominant mode is associated with the eigenfunction $\phi_{01}^{(1)} > 0$, Eq. 13, which is radially symmetric. This implies that nonradially symmetric initial temperature distributions eventually tend to exhibit radially symmetry, and this dynamical behavior is reflected in the configuration of sensor placement shown in Figure 3a.

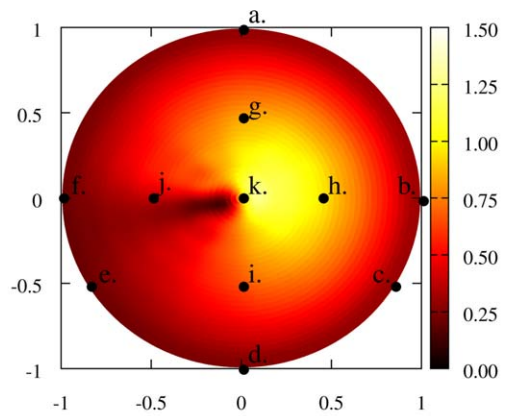

(a) Temperature distribution $z(r, \theta, 0) = z_0(r, \theta)$ and sensor locations $\{a., b., ..., k.\}$

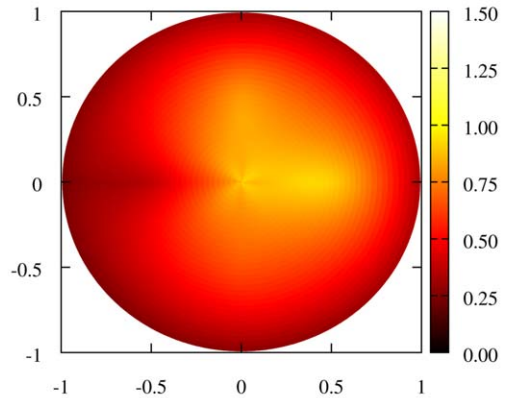

(b) Temperature distribution $\hat{z}(r, \theta, 0) = \hat{z}_0(r, \theta)$ reconstructed using sensor locations $\{a, b, d, f, g, h, i, j, k\}$.

Figure 3. Initial battery temperature distribution $z(r, \theta, 0) = z_0(r, \theta)$ and temperature distribution reconstructed by Delaunay triangulation interpolation method.[31]

[Color figure can be viewed in the online issue, which is available at wileyonlinelibrary.com.]

In terms of the output feedback control problem, the controller design is then considered for the system $\Sigma(A(t), \mathfrak{A}(t)B, I)$. The determination of the input $u(t)$ has two components: first, the stabilization of the state-related generation term $g(t)$, and second, the stabilization of the nonstate-related generation term $q(t)$. For the state-related component, one may consider the finite-time horizon quadratic minimization of the cost functional[30]

$$J(v_0; 0, T, u) = \int_0^T \left(|v(\tau)|^2 + |Ru(\tau)|^2 \right) d\tau + \langle v(T), Qv(T) \rangle \tag{46}$$

The operator $Q \in \mathcal{L}(\mathcal{Z})$ is self-adjoint and nonnegative and $R \in \mathcal{U}$ is coercive. The associated solution is determined in terms of the operator $\Pi(t) \in \mathcal{L}(\mathcal{Z})$ which is the strongly continuous, self-adjoint, nonnegative solution of the differential Riccati equation[30]

$$\dot{\Pi}(t) + (A(t))^* \Pi(t) + \Pi(t) A(t) - \Pi(t) (\mathfrak{A}(t)B) R^{-1} (\mathfrak{A}(t)B)^* \Pi(t) + I = 0 \tag{47}$$

with final time condition $\Pi(T) = Q$. The nonstate-related generation term is accounted for by considering the auxiliary differential equation in terms of $\Gamma(t)$

$$\dot{\Gamma}(t) = [(A(t))^* - \Pi(t)(\mathfrak{A}(t)B)(\mathfrak{A}(t)B)^*] \Gamma(t) + \Pi(t) q(t), \quad \Gamma(T) = 0 \tag{48}$$

Together, the finite time optimization problem has the minimizing solution related by the feedback formula

$$u_{\min}(t) = -R^{-1} (\mathfrak{A}(t)B)^* (\Pi(t) v(t)) - (\mathfrak{A}(t)B)^* \Gamma(t) \tag{49}$$

Given that the interpolated temperature field provides a good approximation to the actual one, the state $\hat{v}(t) \approx v(t)$ can be utilized in the feedback formula in Eq. 49 to stabilize the system.

There are two important issues to be discussed before proceeding to the realization of the battery control problem in the following section. First, one can note that the generation terms $g(t)$ and $q(t)$ which are the sources of instability in the system effect all of the modes (m, n) of the system. For the state-related generation term $g(t)$, this instability can be seen directly from Eq. 29 where $\lambda_{mn}(t) = -\alpha_{m,n}^2 + g(t)$. As $g(t)$ is bounded, there exists a finite-set of modes which are unstable, that is, the set (m_u, n_u) such that $\lambda_{m_u, n_u} > 0$. Then, a finite-dimensional controller in terms of $\Pi(t)$ in Eqs. 47–49 of order $m_u + n_u$ can be designed to stabilize these modes. However, the nonstate-related generation term $q(t)$, while also bounded and only dominant in the first few modes, contributes to all of (m, n). Consequently, it is not feasible to obtain a finite-dimensional controller in terms of $\Gamma(t)$ from Eq. 48 such that the control law in Eq. 49 will completely negate the

contribution of the nonstate-related generation term. However, in the following section, we will demonstrate that it is possible to mitigate the growth in temperature by using a low-order finite-dimensional controller based on the infinite-dimensional system representation of the battery control problem with boundary input.

Numerical Simulation and Case Studies

This section deals with the application of the closed loop output feedback controller design based on the infinite-dimensional systems representation of the Li-ion battery boundary controlled thermal regulation problem. A set of case studies will be considered to demonstrate the effect of controller tuning on the overall behavior of the temperature dynamics in the closed loop system. The general approach will be to utilize the plant model provided in the Model Description section, and employ a finite-dimensional output feedback controller based on the formulation presented in the previous section. We consider a battery system with a 1.5 Amp hour capacity discharged at a rate of 1C where the dynamics of the plant model is based on the modal decomposition of the PDE system in Eqs. 4–6 into a finite-dimensional system.[8] The system parameters are listed in Table 4. The open loop dimensionless temperature distribution $z(r,\theta,t)$ of the battery at select time instances is shown in Figure 4 starting from the initial distribution shown in Figure 3a. The total entropy change is shown in Figure 1d. One can see the effect on the battery temperature due to the generation terms $g(t)$ and $q(t)$ which are dependent on the total entropy change as the battery is discharged.

The output feedback controller design is based on the method proposed in the previous section. First, the temperature measurement locations shown in Figure 3a are used to reconstruct the temperature distribution $\hat{z}(r,\theta,t)$ by interpolation as in Figure 3b. The first-order control law corresponds to the single unstable mode of the system at $m=0, n=1$, that is, $\lambda(t)_{01} > 0$ and $\lambda(t)_{mn} < 0$ for all $m \geq 1, n \geq 2,\ t \in [0,T]$. The quadratic minimization problem

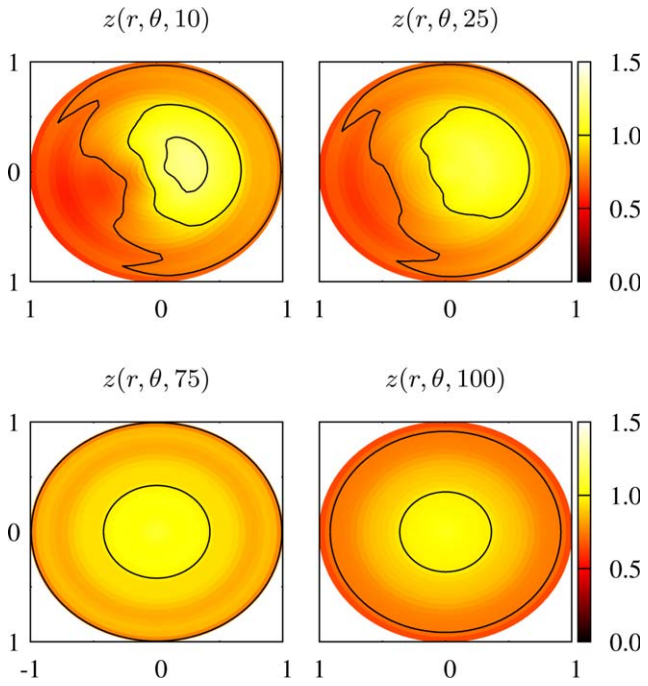

Figure 4. Open loop temperature distributions.

[Color figure can be viewed in the online issue, which is available at wileyonlinelibrary.com.]

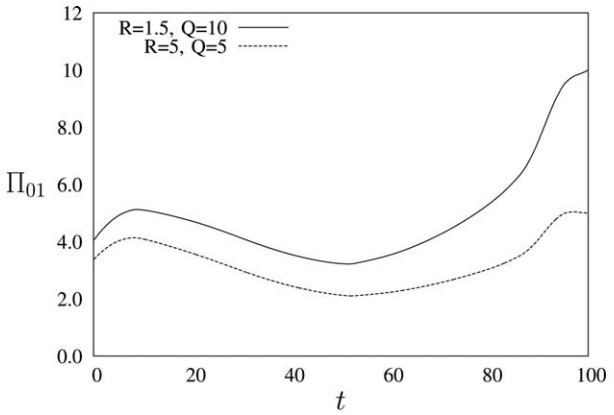

(a) Solution $\Pi_{01}(t)$ of the differential Riccati equation for $R = 1.5, Q = 10$ and $R = 5, Q = 5$.

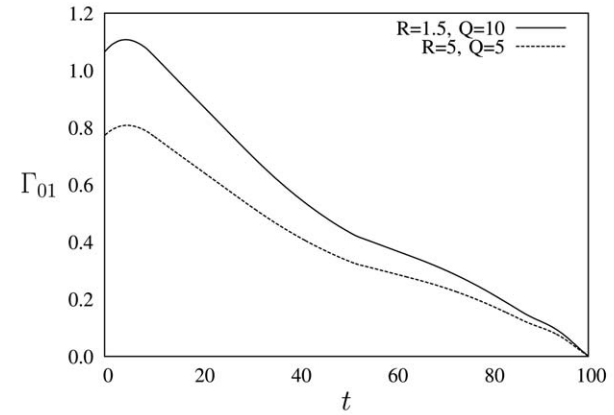

(b) Solution $\Gamma_{01}(t)$ of the auxiliary equation for $R = 1.5, Q = 10$ and $R = 5, Q = 5$.

Figure 5. Solutions $\Pi_{01}(t)$ and $\Gamma_{01}(t)$ under controller tuning parameters.

given in Eqs. 46–48 is solved to obtain the feedback formula in Eq. 49. The input $u(t) \in \mathbb{R}$ is explicitly given by

$$
\begin{aligned}
u_{\min}(t) &= -R^{-1}\Pi_{01}(t)\langle(\mathfrak{A}(t)B)\hat{v},\psi_{01}\rangle\phi_{01} \\
&\quad -\Gamma_{01}(t)\langle(\mathfrak{A}(t)B),\psi_{01}\rangle\phi_{01} \\
&= -D^{-1}\left[R^{-1}\Pi_{01}(t)\left(\int_{-\pi}^{\pi}\int_{0}^{1}(\mathfrak{A}(t)B)\hat{z}\psi_{01}drd\theta\right)\phi_{01}\right. \\
&\quad \left.+\Gamma_{01}(t)\left(\int_{-\pi}^{\pi}\int_{0}^{1}(\mathfrak{A}(t)B)\psi_{01}drd\theta\right)\phi_{01}\right]
\end{aligned}
\tag{50}
$$

where $D = 1 - R^{-1}\Pi_{01}\left(\int_{-\pi}^{\pi}\int_{0}^{1}(\mathfrak{A}(t)B)B\psi_{01}drd\theta\right)\phi_{01}$. The function $\Pi_{01}(t) \in \mathbb{R}$ is the solution of the scalar form of the

Table 1. Cases 1 and 2: Measurement and Control Parameters

Parameter	Setting
Number of sensors	9
Sensor locations	a,b,d,f,g,h,i,j,k
Centre of input	$\theta_{ctr} = \pi/2$
Boundary input region	$r = 1,\ \theta \in (\pi/4, 3\pi/4)$
Shape parameter	$K_1 = 20$
Case 1: Controller tuning	$R = 1.5, Q = 10$
Case 2: Controller tuning	$R = 5, Q = 5$

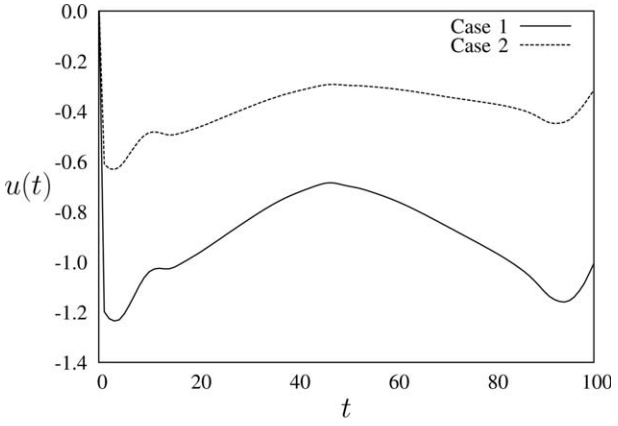

(a) Input profiles for Case 1 and Case 2.

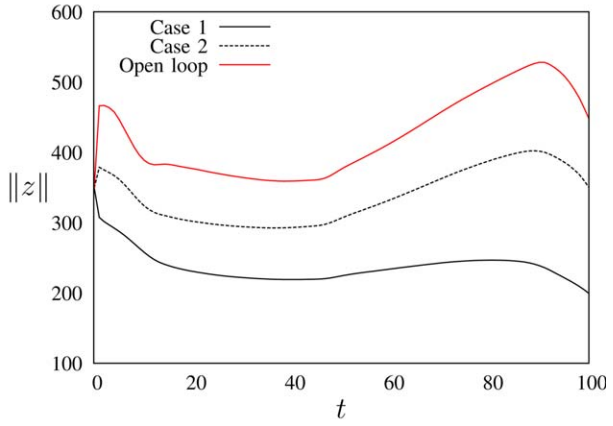

(b) System energy profiles for Case 1, Case 2, and the open loop system.

Figure 6. Input and energy profiles for Cases 1 and 2.

[Color figure can be viewed in the online issue, which is available at wileyonlinelibrary.com.]

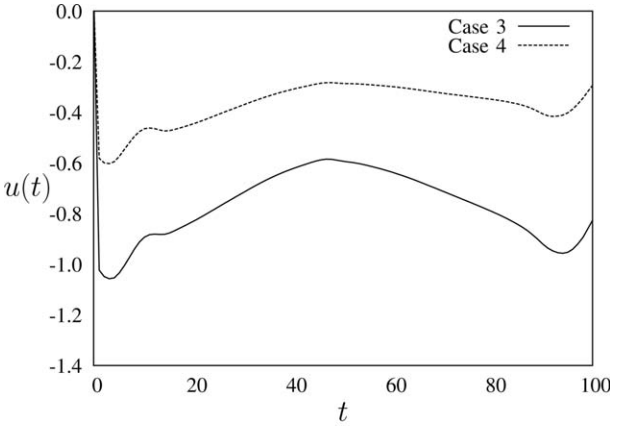

(a) Input profiles for Case 3 and Case 4.

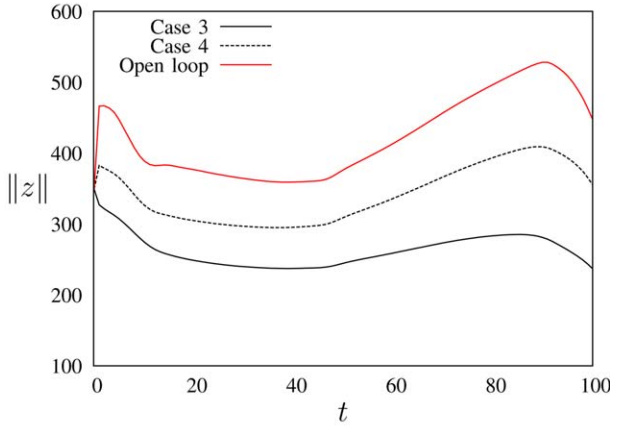

(b) System energy profiles for Case 3, Case 4, and the open loop system.

Figure 7. Input and energy profiles for Cases 3 and 4.

[Color figure can be viewed in the online issue, which is available at wileyonlinelibrary.com.]

differential Riccati equation in Eq. 47 corresponding to the first mode of the PDE system, and similarly $\Gamma_{01}(t) \in \mathbb{R}$ is the solution of the scalar form of the auxiliary equation in Eq. 48. Each of these solutions shown in Figures 5a and 5b, respectively, are dependent on the controller tuning parameters $Q \in \mathbb{R}$ and $R \in \mathbb{R}$.

The following case studies are considered to examine the effect of sensor placement, number of sensors, and controller tuning parameters on the closed loop feedback system. Cases 1 and 2 use the same sensor number and placement, while the controller used in Case 1 is relatively more aggressive controller than the controller used in Case 2. The second set of cases Cases 3 and 4 use a reduced number of sensors in a different configuration than Cases 1 and 2.

Table 2. Cases 3 and 4: Measurement and Control Parameters

Parameter	Setting
Number of sensors	4
Sensor locations	a,c,e,k
Centre of input	$\theta_{\text{ctr}} = \pi/2$
Boundary input region	$r = 1,\ \theta \in (\pi/4, 3\pi/4)$
Shape parameter	$K_1 = 20$
Case 3: Controller tuning	$R = 1.5, Q = 10$
Case 4: Controller tuning	$R = 5, Q = 5$

Cases 1 and 2

The closed loop feedback systems for Cases 1 and 2 were simulated using the sensor and tuning parameters in Table 1. The boundary input profiles for each set of tuning parameters is shown in Figure 6a. As expected, the tuning parameters used in the control design for Case 1 resulted in a relatively more aggressive input profile compared to the input profile used in the control design for Case 2. The battery temperature distribution and the reconstructed temperature distribution at select time instances for Case 1 is shown in Figure 8a (cf. Figure 4) where the influence of the input over the region of the boundary centered at $\pi/2$ on the whole distribution can be clearly seen. The overall temperature distribution and dynamical behavior is captured by the interpolation scheme using the number and configuration of sensors. The total system energy $E = ||z(r, \theta, t)||$ profiles for Case 1, Case 2, and for the open system, are shown in Figure 6b. One can see the growth in overall system energy in the open loop system due to the exothermic heat generation, and the energy profiles of the closed loop systems each show a lower total system energy profile. At the end of the discharge cycle, $E \approx 200$ for the controller designed using the parameters in Case 1, compared to $E \approx 450$ for the open loop system. While the controller is not able to completely dissipate the heat generated by the exothermic chemical reactions producing the current in the battery, the maximum temperature and

overall temperature variance is reduced by use of the output feedback controller with boundary actuation. As previously discussed, it is not possible to completely negate the influence of the nonstate generation term $q(t)$ as it affects the infinite-number modes. However, increasing the order of the controller will further mitigate the effect of this generation term.

Cases 3 and 4

In Cases 3 and 4, the number of sensors were reduced relative to the number used in Cases 1 and 2, and the placement of the sensors was also altered (cf. Figure 3a). The sensor and tuning parameters for each case are listed in Table 2, the boundary input profiles are shown in Figure 7a, the energy profiles are shown in Figure 7b, and the battery temperature distribution and the reconstructed temperature

Table 3. Nomenclature

Symbol	Description
C_p	Specific heat capacity (J kg $^{-1}$K^{-1})
F	Faraday constant (96, 485C $\cdot$ mol $^{-1}$)
h	Heat transfer coefficient (W $\cdot$ m^{-1}K^{-1})
i	Current (Amps $\cdot$ m^{-2})
K0	Thermal conductivity (W $\cdot$ m^{-1}K^{-1})
n_R	Reaction charge number
Q	Heat generation (W $\cdot$ m^{-3})
S_Δ	Entropy change (J $\cdot$ mol $^{-1}$ $\cdot$ K^{-1})
V	Volume (m3)
x	Electrode averaged ion concentration
Z	Temperature (K)
Z_a	Ambient temperature (K)
ρ	Density (kg $\cdot$ m^{-3})
σ_{con}	Electrical conductivity (S $\cdot$ m^{-1})

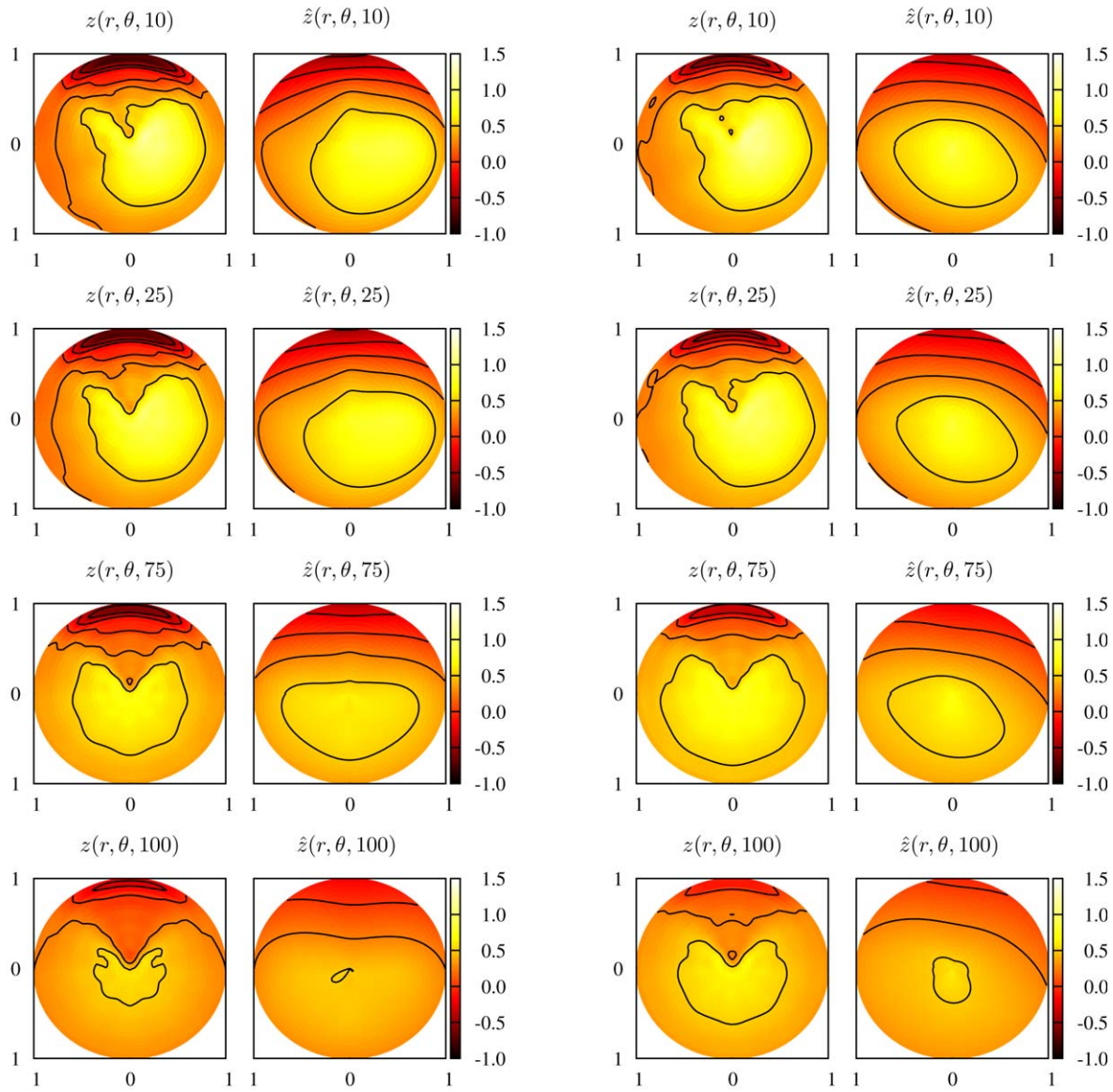

(a) Closed loop temperature distributions for Case 1

(b) Closed loop temperature distributions for Case 3

Figure 8. Closed loop temperature distributions for Cases 1 and 3.

(Left column) Actual temperature $z(r,\theta,t)$. (Right column) Reconstructed temperature $\hat{z}(r,\theta,t)$. [Color figure can be viewed in the online issue, which is available at wileyonlinelibrary.com.]

Table 4. Physical Properties

Componet	Thickness (μm)	Proportion $p^{(i)}$ (%)	$p^{(i)}\rho^{(i)}$	$p^{(i)}K_0^{(i)}$	$p^{(i)}C_p^{(i)}$	$p^{(i)}\sigma^{(i)}$
$LiCoO_2$	92	0.42	962	0.78	0.49	0.000042
LiC_6	87	0.39	1962	1.95	0.27	0.000039
Al	10	0.045	122	9.0	0.039	1.71
Cu	10	0.045	405	17.1	0.017	2.70
Separator	22	0.10	120	0.10	0.7	–
Total	221	1.00	ρ=3571	K_0=29.93	C_p=1.522	σ=4.4100081

distribution at select time instances for Case 3 are shown in Figure 8b. Once again, the input and energy profiles reflect the difference in tuning parameters for each of the controllers corresponding to Cases 1 and 2. Comparison of the temperature distributions in Figures 8a and 8b illustrates how changing the number and the configuration of sensors influences the reconstruction of the temperature distribution. The sensor placements, measurements taken, and the resulting interpolation in Case 1 is better able to capture the nonsymmetric temperature distribution of the disk compared to the interpolation based on the sensor locations in Case 3. As previously mentioned, the temperature tends to an axisymmetric distribution over time as the battery is discharged, and the reconstructed distributions for Cases 1 and 3 become more similar. One can notice that the input and energy profiles for Cases 2 and 4, having the same tuning parameters, are closely aligned. On the other hand, the input and the resulting energy profiles for Cases 1 and 3 show a greater difference. At the end of the discharge cycle, the energy is $E \approx 225$ for the controller designed using the parameters in Case 3 (compared to $E \approx 200$ for Case 1), and is $E \approx 350$ for each of the controllers corresponding to Cases 2 and 4. This suggests that there may be a relationship between aggressive controller tuning and the number and/or placement of sensors. In other words, the input to the system generated by the controller is influenced by the number and the placement of sensors (and subsequently, the accuracy of the temperature distribution reconstruction), but this influence is diminished for less aggressive control designs.

Summary

This article considered the thermal regulation problem for a Li-ion battery by output feedback control and boundary control actuation. The model of the battery temperature dynamics was given by a nonhomogeneous parabolic partial differential equation (PDE) on a 2-D spatial domain with angular and radial coordinates. The heat generation during battery discharge is attributed to the underlying exothermic electrochemical reactions that appear as state-related and nonstate-related generation terms in the model. Several key challenges in the output feedback model-based controller design were addressed in this work. First, the dependence of the state on time-varying system parameters yielded a nonautonomous infinite-dimensional system with time-varying nonhomogeneous generation term. Second, the restriction of the input along a portion of the battery domain boundary required the reformulation of the boundary control problem into a suitable form. Third, the compensator design problem was considered and the closed loop system for the observer-based optimal boundary control system was demonstrated to be stable under appropriate design of the observer and controller gain operators using the separation principle. Finally, the outback feedback control problem based on state measurement and interpolation of the temperature field was provided and the numerical simulation results for several case studies were presented.

Literature Cited

1. Lu L, Han X, Li J, Hua J, Ouyang M. A review on the key issues for lithium-ion battery management in electric vehicles. *J Power Sources*. 2013;226:272 – 288.
2. Balakrishnan P, Ramesh R, Kumar TP. Safety mechanisms in lithium-ion batteries. *J. Power Sources* 2006;155(2):401 – 414.
3. Wang Q, Ping P, Zhao X, Chu G, Sun J, Chen C. Thermal runaway caused fire and explosion of lithium ion battery. *J Power Sources* 2012;208:210 – 224.
4. Gu W, Wang C. Thermal-electrochemical modeling of battery systems. *J Electrochem Soc*. 2000;147(8):2910–2922.
5. Chen S, Wan C, Wang Y. Thermal analysis of lithium-ion batteries. *J Power Sources*. 2005;140(1):111 – 124.
6. Bandhauer T, Garimella S, Fuller T. A critical review of thermal issues in lithium-ion batteries. *J Electrochem Soc*. 2011;158(3):R1–R25.
7. Rao Z, Wang S. A review of power battery thermal energy management. *Renewable Sustainable Energy Rev*. 2011;15(9):4554 – 4571.
8. Ray WH. *Advanced Process Control*. New York: McGraw-Hill, 1981.
9. Atwell JA, King BB. Proper orthogonal decomposition for reduced basis feedback controllers for parabolic equations. *Math Comput Model*. 2001;33:1–19.
10. Smyshlyaev A, Krstic M. Explicit formulae for boundary control of parabolic PDEs. *Lecture Notes Control Inf Sci*. 2004;301:231–249.
11. Krstic M. *Boundary Control of PDEs: A Course on Backstepping Designs*. Philadelphia, PA: Society for Industrial and Applied Mathematics, 2008.
12. Christofides PD, Daoutidis P. Finite-dimensional control of parabolic PDE systems using approximate inertial manifolds. *J Math Anal Appl*. 1997;216:398–420.
13. Christofides PD. *Nonlinear and Robust Control of PDE Systems: Methods and Applications to Transport-Reaction Processes*. Boston: Birkhäuser, 2001.
14. Orlov Y, Utkin V. Sliding mode control in indefinite-dimensional systems. *Automatica*. 1987;23(6):753 – 757.
15. Curtain RF, Zwart H. *An Introduction to Infinite-Dimensional Linear Systems Theory*. New York, NY: Springer-Verlag, 1995.
16. Garcia MR, Vilas C, Banga JR, Alonso AA. Exponential observers for distributed tubular (bio)reactors. *AIChE J*. 2008;54(11):2943–2956.
17. Pazy A. *Semigroups of Linear Operators and Applications to Partial Differential Equations*. New York: Springer-Verlag, 1983.
18. McOwen R. *Partial Differential Equations: Methods and Applications*, 2nd ed. Upper Saddle River, NJ, USA: Prentice Hall. 2002.
19. Tanabe H. *Functional Analytic Methods for Partial Differential Equations*. New York: Marcel Dekker, 1997.
20. Evans L. *Partial Differential Equations*. Providence, R.I., USA: American Mathematical Society, 1998.
21. Williford RE, Viswanathan VV, Zhang JG. Effects of entropy changes in anodes and cathodes on the thermal behavior of lithium ion batteries. *J Power Sources*. 2009;189(1):101 – 107.
22. Reynier Y, Graetz J, Swan-Wood T, Rez P, Yazami R, Fultz B. Entropy of Li intercalation in Li_x CoO_2. *Phys Rev B*. 2004;70: 174304.
23. Reynier Y, Yazami R, Fultz B. Thermodynamics of lithium intercalation into graphites and disordered carbons. *J Electrochem Soc*. 2004;151(3):A422–A426.
24. Jeon DH, Baek SM. Thermal modeling of cylindrical lithium ion battery during discharge cycle. *Energy Conversion Manage*. 2011; 52(89):2973 – 2981.

25. Delmon D, Froment G. *Catalyst Deactivation*. Amsterdam, Netherlands: Elsevier Science, 1987.
26. Weitsman Y. Diffusion with time-varying diffusivity, with application to moisture-sorption in composites. *J Compos Mater*. 1976; 10(3):193–204.
27. Forgez C, Do DV, Friedrich G, Morcrette M, Delacourt C. Thermal modeling of a cylindrical LiFePO4/graphite lithium-ion battery. *J Power Sources*. 2010;195(9):2961 – 2968.
28. Smyshlyaev A, Krstic M. Backstepping observers for a class of parabolic PDEs. *Syst Control Lett*. 2005;54(7):613–625.
29. Ramdani K, Tucsnak M, Weiss G. Recovering the initial state of an infinite-dimensional system using observers. *Automatica*. 2010; 46(10):1616–1625.
30. Bensoussan A, Prato GD, Delfour M, Mitter S. *Representation and Control of Infinite Dimensional Systems*. Boston: Birkhäuser, 2007.
31. Berg Md, Cheong O, Kreveld Mv, Overmars M. *Computational Geometry: Algorithms and Applications*, 3rd ed. Santa Clara, CA: Springer-Verlag, 2008.

Appendix

A proof of Proposition 1

It is standard to prove (i) and (ii), and for brevity we only provide an outline of the procedure (e.g., see Ref. 30). The entropy-related generation term $g(t)$ is bounded by definition $||g(t)|| \le k_g = \sup\{||g(t)|| : t \in [0,T]\}$, and the operator $A(t)$ in Eq. 26 can be seen as a perturbation of an autonomous operator $A(t)=A+g(t)$, where $g(t)v \in C([0,T];\mathcal{Z})$. The semigroup $S_A(t)$ generated by A is exponentially stable, $\|S_A(t)\| \le Me^{\omega t}$, $\omega_0 := \sup_{m\ge 0, n\ge 1}\left(-\alpha_{mn}^2\right) \le \omega$, where M is a generic positive constant, $\omega > 0$. Then, for $z \in \mathcal{Z}$, $z(t)=S(t)z_0+\int_0^t S(t-\tau)(g(\tau)z(\tau))d\tau$ and application of Gronwall's lemma yields the bound on the evolution operator

$$||U(t,s)|| \le Me^{(\omega+k_g)(t-s)}$$

The uniform continuity in the operator topology can be demonstrated considering the approximation $U_k(t,s)$, and application of the contraction mapping principle (method of successive approximations), one can show that for any $z \in \mathcal{Z}$, $\lim_{k\to\infty} U_k(t,s)z = U(t,s)z$ uniformly.

The first identity $U(t,t)=I$ is easily seen by inspection. The second identity can directly verified where for $0 \le s \le r \le t \le T$

$$\begin{aligned}
U(t,r)U(r,s)v &= \sum_{m=0,n=1}^{\infty} e^{\int_r^t \lambda_{mn}(\tau)d\tau}\Big\langle \sum_{k,l=0}^{\infty} e^{\int_s^r \lambda_{kl}(\tau)d\tau}\langle v,\psi_{kl}\rangle\phi_{kl},\psi_{mn}\Big\rangle\phi_{mn} \\
&= \sum_{m=0,n=1}^{\infty} e^{\int_r^t \lambda_{mn}(\tau)d\tau}\left(\int_\Omega \sum_{k,l=0}^{\infty} e^{\int_s^r \lambda_{kl}(\tau)d\tau}\left(\langle v,\psi_{kl}^{(1)}\rangle\phi_{kl}^{(1)}+\langle v,\psi_{kl}^{(2)}\rangle\phi_{kl}^{(2)}\right)\begin{pmatrix}\psi_{mn}^{(1)}\\ \psi_{mn}^{(2)}\end{pmatrix}d\theta dr\right)\phi_{mn} \\
&= \sum_{m=0,n=1}^{\infty} e^{\int_r^t \lambda_{mn}(\tau)d\tau}\left(\int_\Omega \sum_{k,l=0}^{\infty} e^{\int_s^r \lambda_{kl}(\tau)d\tau}\begin{pmatrix}\langle v,\psi_{kl}^{(1)}\rangle\phi_{kl}^{(1)}\psi_{mn}^{(1)}+\langle v,\psi_{kl}^{(2)}\rangle\phi_{kl}^{(2)}\psi_{mn}^{(1)}\\ \langle v,\psi_{kl}^{(1)}\rangle\phi_{kl}^{(1)}\psi_{mn}^{(2)}+\langle v,\psi_{kl}^{(2)}\rangle\phi_{kl}^{(2)}\psi_{mn}^{(2)}\end{pmatrix}d\theta dr\right)\phi_{mn}
\end{aligned}$$

Note that double series terms within the inner product are equal to zero for all $k \ne m$ and $l \ne n$, and equal to 1 for each $k=m$ and $l=n$, due to the orthogonality of the eigenfunctions. Also, for every $k,m=0,1,2,\ldots$, $l,n=1,2,3\ldots$, the inner product of the cross terms $\int_\Omega \langle v,\psi_{kl}^{(2)}\rangle\phi_{kl}^{(2)}\psi_{mn}^{(1)}drd\theta=0$ and $\int_\Omega \langle v,\psi_{kl}^{(1)}\rangle\phi_{kl}^{(1)}\psi_{mn}^{(2)}drd\theta=0$, such that

$$\begin{aligned}
U(t,r)U(r,s)v &= \sum_{m=0,n=1}^{\infty} e^{\int_r^t \lambda_{mn}(\tau)d\tau+\int_s^r \lambda_{mn}(\tau)d\tau}\begin{pmatrix}\langle v,\psi_{mn}^{(1)}\rangle\\ \langle v,\psi_{mn}^{(2)}\rangle\end{pmatrix}\phi_{mn} \\
&= \sum_{m=0,n=1}^{\infty} e^{\int_s^t \lambda_{mn}}(\tau)d\tau\langle v,\begin{pmatrix}\psi_{mn}^{(1)}\\ \psi_{mn}^{(2)}\end{pmatrix}\rangle\phi_{mn} = U(t,s)v
\end{aligned}$$

The second identity in (iii) can also be directly verified as follows

$$\begin{aligned}
\frac{\partial U(t,s)}{\partial t} &= \frac{\partial}{\partial t}\sum_{m=0,n=1}^{\infty} e^{\int_s^t \lambda_{mn}(\tau)d\tau}\langle v,\psi_{mn}\rangle\phi_{mn} \\
&= -\sum_{m=0,n=1}^{\infty}\left(\alpha_{m,n}^2-g(t)\right)e^{\int_s^t \lambda_{mn}(\tau)d\tau}\langle v,\psi_{mn}\rangle\phi_{mn} \\
&= \sum_{m=0,n=1}^{\infty}\lambda_{mn}(t)e^{\int_s^t \lambda_{mn}(\tau)d\tau}\langle v,\psi_{mn}\rangle\phi_{mn} = A(t)U(t,s)
\end{aligned}$$

From the other side we have

$$\begin{aligned}
A(t)U(t,s) &= \sum_{m=0,n=1}^{\infty}\lambda_{mn}(t)\Big\langle\sum_{k,l=0}^{\infty} e^{\int_s^t \lambda_{kl}(\tau)d\tau}\langle\cdot,\psi_{kl}\rangle\phi_{kl},\psi_{mn}\Big\rangle\phi_{mn} \\
&= \sum_{m=0,n=1}^{\infty}\lambda_{mn}(t)\left(\int_\Omega\sum_{k,l=0}^{\infty} e^{\int_s^t \lambda_{kl}(\tau)d\tau}\left(\langle\cdot,\psi_{kl}^{(1)}\rangle\phi_{kl}^{(1)}\right.\right. \\
&\quad \left.\left.+\langle\cdot,\psi_{kl}^{(2)}\rangle\phi_{kl}^{(2)}\right)\begin{pmatrix}\psi_{mn}^{(1)}\\ \psi_{mn}^{(2)}\end{pmatrix}d\theta dr\right)\phi_{mn}
\end{aligned}$$

Similar as in the previous case, we have that

$$\begin{aligned}
A(t)U(t,s) &= \sum_{m=0,n=1}^{\infty}\lambda_{mn}(t)\Big\langle\sum_{k,l=0}^{\infty} e^{\int_s^t \lambda_{kl}(\tau)d\tau}\langle\cdot,\psi_{kl}\rangle\phi_{kl},\psi_{mn}\Big\rangle\phi_{mn} \\
&= \sum_{m=0,n=1}^{\infty}\lambda_{mn}(t)e^{\int_s^t \lambda_{mn}(\tau)d\tau}\langle\cdot,\psi_{mn}\rangle\phi_{mn} = \frac{\partial}{\partial t}U(t,s)
\end{aligned}$$

A proof of Proposition 2

From the definition of the operator in Eqs. 29 and 30, we have that

$$Bu=\sum_{m=0,n=1}^{\infty}\langle B,\psi_{mn}\rangle\phi_{mn}u,$$

$$U(t,s)\ Bu=\sum_{m=0,n=1}^{\infty}e^{\int_s^t\lambda_{mn}(\eta)d\eta}\langle B,\psi_{mn}\rangle\phi_{mn}u$$

$$U(t,s)z=\sum_{m=0,n=1}^{\infty}e^{\int_0^t\lambda_{mn}(\eta)d\eta}\langle z,\psi_{mn}\rangle\phi_{mn}$$

$$U(t,s)\mathfrak{A}Bu=\sum_{m=0,n=1}^{\infty}e^{\int_s^t\lambda_{mn}(\eta)d\eta}\langle\mathfrak{A}(s)B,\psi_{mn}\rangle\phi_{mn}u$$

The term involving the derivative of the input is expanded as

$$\int_0^t U(t,\tau)B\dot{u}(\tau)d\tau=\int_0^t\sum_{m=0,n=1}^{\infty}e^{\int_\tau^t\lambda_{mn}(\eta)d\eta}\langle B,\psi_{mn}\rangle\phi_{mn}\dot{u}(\tau)d\tau$$

$$=\sum_{m=0,n=1}^{\infty}\left(\int_0^t e^{-\alpha_{mn}^2(t-\tau)+G(t)-G(\tau)}\langle B,\psi_{mn}\rangle\dot{u}(\tau)d\tau\right)\phi_{mn}$$

$$=\sum_{m=0,n=1}^{\infty}\left(e^{-\alpha_{mn}^2t+G(t)}\int_0^t e^{\alpha_{mn}^2\tau-G(\tau)}\dot{u}(\tau)d\tau\right)\langle B,\psi_{mn}\rangle\phi_{mn}$$

$$=\sum_{m=0,n=1}^{\infty}\left[\left(u(t)-u(0)e^{\int_0^t\lambda_{mn}(\eta)d\eta}\right)\right.$$

$$\left.+\int_0^t\lambda_{mn}(\tau)e^{\int_\tau^t g(\eta)d\eta}u(\tau)d\tau\right]\langle B,\psi_{mn}\rangle\phi_{mn}$$

Combining Eq. 32 and the expression above, the mild solution is given by

$$z(t)=\sum_{m=0,n=1}^{\infty}\left(u(t)-u(0)e^{\int_0^t\lambda_{mn}(\eta)d\eta}\right)\langle B,\psi_{mn}\rangle\phi_{mn}$$
$$+\sum_{m=0,n=1}^{\infty}e^{\int_0^t\lambda_{mn}(\eta)d\eta}\langle z_0,\psi_{mn}\rangle\phi_{mn}$$
$$-\sum_{m=0,n=1}^{\infty}\left[\left(u(t)-u(0)e^{\int_0^t\lambda_{mn}(\eta)d\eta}\right)\right.$$
$$\left.+\int_0^t\lambda_{mn}(\tau)e^{\int_\tau^t g(\eta)d\eta}u(\tau)d\tau\right]\langle B,\psi_{mn}\rangle\phi_{mn}$$
$$+\int_0^t\sum_{m=0,n=1}^{\infty}e^{\int_\tau^t\lambda_{mn}(\eta)d\eta}\langle\mathfrak{A}(\tau)B,\psi_{mn}\rangle\phi_{mn}u(\tau)d\tau$$
$$+\int_0^t U(t,\tau)q(\tau)d\tau$$

Rearranging terms gives that

$$z(t)=U(t,0)z_0+\int_0^t U(t,\tau)q(\tau)d\tau$$
$$+\sum_{m=0,n=1}^{\infty}\int_0^t e^{\int_\tau^t\lambda_{mn}(\eta)d\eta}u(\tau)[\langle\mathfrak{A}(\tau)B,\psi_{mn}\rangle$$
$$-\lambda_{mn}(\tau)\langle B,\psi_{mn}\rangle]\phi_{mn}d\tau$$

To demonstrate that the above equation is well defined for every $u(t)\in L^2([0,T];\mathcal{U})$, recall that $g(t),q(t)\in L^2([0,T];\mathcal{Z})$, $B\in L^2(\Omega)$, $D(\mathfrak{A}(t))\subset L^2(\Omega)$. Moreover, from Figure 1d, the generation term $g(t)\le g(0)+Mt$ for all $0\le\tau\le s\le T<\infty$, where M is a finite positive constant and $g(0)$ is the initial generation. Note that the operator $\mathfrak{A}(t)$ defined in Eq. 23 can be represented as $\mathfrak{A}(t)=\mathfrak{A}+g(t)$ such that $\mathfrak{A}B=b_{\mathrm{ctr}}(\theta)(4+\mu(\theta)/(2\beta+1)$ and $g(t)B=g(t)b_{\mathrm{ctr}}(\theta)r^2/(2\beta+1)$, from Eq. 11, and $\lambda_{mn}(t)=-\alpha_{mn}^2+g(t)$, from Eq. 29. Then, by substituting these terms into the above equation yields

$$z(t)=U(t,0)z_0+\int_0^t U(t,\tau)q(\tau)d\tau$$
$$+\sum_{m=0,n=1}^{\infty}\int_0^t e^{\int_\tau^t\lambda_{mn}(\eta)d\eta}u(\tau)[\langle\mathfrak{A}B,\psi_{mn}\rangle$$
$$+\alpha_{mn}^2\langle B,\psi_{mn}\rangle]\phi_{mn}d\tau$$

Integrating over $t\in[0,T]$ and appealing to the Hölder inequality, we have that

$$\left|\int_0^t e^{\int_\tau^t\lambda(\eta)d\eta}u(\tau)d\tau\right|^2\le\frac{1}{2}\sqrt{\frac{\pi}{M}}e^{\frac{\left(-\alpha_{mn}^2+g(0)+Mt\right)^2}{M}}$$
$$\left[erf\left(\frac{\alpha_{mn}^2-g(0)}{\sqrt{M}}\right)+erf\left(\frac{-\alpha_{mn}^2+g(0)+Mt}{\sqrt{M}}\right)\right]\int_0^t|u(\tau)|^2d\tau$$

where $erf(x)=2/\sqrt{\pi}\int_0^x\exp\left(-\xi^2\right)d\xi$ is the error function. As $-1\le erf(x)\le 1$ for all $x\in\mathbb{R}$, then we have that

$$\left|\int_0^t e^{\int_\tau^t\lambda(\eta)d\eta}u(\tau)d\tau\right|^2\le\frac{1}{2}\sqrt{\frac{\pi}{M}}\exp\left\{\frac{\left(-\alpha_{mn}^2+g(0)+MT\right)^2}{M}\right\}$$
$$\int_0^t|u(\tau)|^2d\tau$$

for all $0\le\tau\le t\le T$, and therefore $z(t)$ is well defined for every $u(t)\in L^2([0,T];\mathcal{U})$.

Manuscript received Feb. 19, 2013, and revision received Jun. 13, 2013.